Electromagnetic Radiation in the Tamm Problem

C.W. James

ECAP, Friedrich-Alexander University of Erlangen-Nuremberg, Erwin-Rommel-Str. 1, 91058 Erlangen, Germany

Abstract. The 'Tamm Problem' is the calculation of the electromagnetic fields from a single particle travelling a finite distance at superluminal velocities in a medium. It was first addressed by Frank Tamm in 1939 as an extension to the Frank-Tamm theory of Vavilov-Cherenkov radiation from a particle moving an infinite distance in a medium. It is exactly the problem which must be solved in order to calculate the radio-emission from high-energy particle cascades simulated by numerical (Monte Carlo) methods, as is performed by the codes REAS, COREAS, and ZHAireS in the case of extensive air showers, and ZHS for cascades in a dense medium such as ice or the Lunar regolith. Despite its importance, the commonly-used solutions to the radiated fields in the Tamm problem — the 'ZHS' approach and 'endpoints' formalism — are not exact solutions, and are only known to be correct in the far-field and away from the Cherenkov angle. In this contribution, an exact solution to the Tamm problem is presented in the form of a numerically-evaluable integral. Using this exact expression, the regimes of applicability of the ZHS and endpoints approach are evaluated.

Keywords: Vavilov-Cherenkov radiation, radio detection, cosmic rays, electromagnetic radiation
PACS: 41.60.-m, 41.60.Ap, 41.60.Bq, 41.60.Dk

1. INTRODUCTION

The theory of Vavilov-Cherenkov radiation was initially developed by Frank and Tamm in 1937 [1], who calculated the radiated power in the case of a particle moving an infinite distance in a medium at a constant, superluminal velocity. Tamm's extension of the problem to the more physical case of a finite particle track in 1939 [2] is of much more interest in the radio-detection of high-energy particles. For the case of extensive air-showers, and showers in dense media, the typical distances over which a particle's velocity can be considered constant can not be approximated as being infinite on the scale of the observation wavelengths (unlike e.g. the optical regime). The most direct application of Tamm's problem to the radio-detection of high-energy particles is in the calculation of the radiated fields from 'particle tracks' as output by a Monte Carlo simulation of a high-energy particle cascade. In such simulations, the motion of each particle is approximated by a series of 'tracks' over which the particle moves with constant velocity, and the radiated fields are calculated by summing the solution to Tamm's problem for each track. This methodology was first applied to the radio-emission from electromagnetic cascades in ice by Zas, Halzen, and Stanev [3]; their formula for the fields in the Tamm problem is commonly known as the 'ZHS' formula, which will be examined in more detail below; and their code, in various forms, is still in use today (e.g. Ref. [4] for extensive air-showers). Another methodology, now known as the 'endpoints' approach, was developed in a specific form for use in the REAS3 air-shower code [5], and later extended to its current form for applicability in more general radiation problems [6]. The authors of Ref. [6] claimed that neither formula gave the exact solution to the Tamm problem over the full range of track-observer geometries, basing on certain assumptions made during their respective derivations. Since the applicability of the ZHS and endpoint formulations was questioned, debate has been on-going as to the veracity of this claim. However, the ultimate test — a comparison to the true, assumption-less solution — could not be made, because the Tamm problem has never been solved exactly. The derivation of such an exact solution, and an evaluation of these formulae, is the subject of this contribution. In Sec. 2, a sketch of the derivation methods of both the ZHS and endpoint formulae is presented, and their predictions for the radiated electric fields in the Tamm problem are compared over the full range of observer geometries. This in particular highlights their divergent solutions in the near-field. The divergence of these seemingly similar methods then prompts a full calculation of the exact electric fields in the Tamm problem in Sec. 3, and a numerically-integrable result is derived. This allows finally the 'ultimate test' of the ZHS and endpoint approaches to be made in Sec. 4, where the range of applicability of each is finally determined.

Throughout this paper, the convention is used where any vector quantity $\vec{x}$ has normalised component written as $\hat{x} = \frac{1}{|x|}\vec{x}$, and magnitude $|x|$ written simply as x. A dotted quantity — e.g. $\dot{x}$ and $\dot{\vec{x}}$ — always indicates a derivative with respect to time. All formulas presented are in Gaussian c.g.s. units, though all results in plots have been converted to S.I. units.

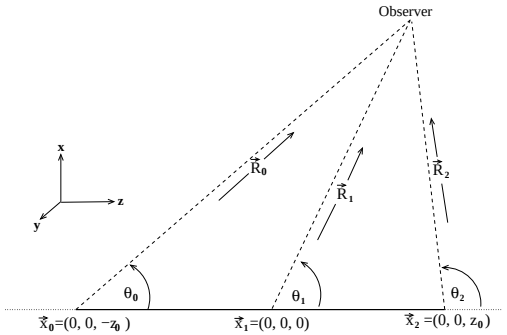

FIGURE 1. Sketch of the geometry and notation used to describe the Tamm problem.

2. ZHS AND ENDPOINTS

The Tamm problem can be described as a particle with charge Q lying stationary at position $\vec{x}_0 = (0,0,-z_0)$ until time $t = -t_0$, at which point it suddenly accelerates to velocity $\vec{v} = (0,0,v)$ (with $\vec{\beta} \equiv \frac{1}{c}\vec{v}$). It travels uniformly until time t_0 ($= z_0/v$) at which point $\vec{x}_2 = (0,0,z_0)$ it suddenly decelerates to zero velocity. This occurs in an infinite uniform (and generally non-magnetic) medium with refractive index n — this geometry is illustrated in Fig. 1. Both the derivation of the ZHS formula presented in Zas, Halzen, and Stanev ('ZHS')[3], and that of the endpoint formulation, treat this problem using the time-domain electric fields $\vec{E}(\vec{x},t)$ derived from the Liénard-Wiechert potentials (see e.g. Ref. [7]):

$$\begin{aligned}\vec{E}(\vec{x},t) &= Q\left[\frac{\hat{R}-n\vec{\beta}}{\gamma^2(1-n\vec{\beta}\cdot\hat{R})^3R^2}\right]_{\rm ret} \\ &+ \frac{Q}{c}\left[\frac{\hat{R}\times[(\hat{R}-n\vec{\beta})\times\dot{\vec{\beta}}]}{(1-n\vec{\beta}\cdot\hat{R})^3R}\right]_{\rm ret} \qquad (1)\end{aligned}$$

where $\vec{R}$ is a vector from the source to the observer, and γ is the usual relativistic factor of $(1-\beta^2)^{-\frac{1}{2}}$. The first term, being proportional to R^{-2}, is often called the 'near-field' term, while the second, proportional to R^{-1}, is the 'far-field' or 'radiation' term. This second term is also proportional to the acceleration $\dot{\vec{\beta}}$, giving rise to the well-known mantra 'accelerated charged particles radiate'. Since the radiated emission in the Tamm problem is of interest, both ZHS and James, Falcke, Huege and Ludwig ('JHFL') discard the near-field term, and proceed to derive the ZHS and endpoint formulas solely from the radiation term. After some relatively short maths, the endpoint solution to the Tamm problem can be shown to be [6]:

$$\begin{aligned}\vec{E}_{\rm ep}(\vec{x},\nu) &= \frac{Q}{c^2}\beta\sin\theta_0\frac{e^{-2\pi i\nu t_0}}{1-n\beta\cos\theta_0}\frac{e^{ikR_0}}{R_0}\hat{E_0} \\ &- \frac{Q}{c^2}\beta\sin\theta_2\frac{e^{2\pi i\nu t_2}}{1-n\beta\cos\theta_2}\frac{e^{ikR_2}}{R_2}\hat{E_2} \qquad (2)\end{aligned}$$

while the ZHS solution is:

$$\begin{aligned}\vec{E}_{\rm zhs}(\vec{x},\nu) &= \frac{Q}{c^2}\beta\sin\theta_1\frac{e^{ikR_1}}{R_1} \\ &\cdot\frac{2\sin[2\pi i\nu(1-n\beta\cos\theta_1)t_0]}{1-n\beta\cos\theta_1}\hat{E_1} \qquad (3)\end{aligned}$$

The field directions are given in each case as:

$$\hat{E_n} = |\hat{R}_n\times(\hat{R}_n\times\hat{\beta})|. \qquad (4)$$

It can readily be seen that the endpoint solution tends towards the ZHS solution in the limit that $\theta_0 = \theta_1 = \theta_2$ and $R_0^{-1} = R_1^{-1} = R_2^{-1}$, in which case the approximation $R_{1\pm1} \approx R_1 \mp ct_0\beta\cos\theta$ can be substituted into Eq. (2) to obtain Eq. (3). Despite this, and despite their very similar derivations, the end-point solution explicitely is derived as the radiation from the implied acceleration at the 'end-points' of the track — i.e. it is bremsstrahlung — while the ZHS formula is usually viewed as giving the radiation from the particle motion, which is more consistent with the picture of Vavilov-Cherenkov radiation.

It at first appears that the ZHS formula is a simple far-field approximation of the endpoints formula. However, it turns out that these approaches produce divergent results in two important limits — when near the Cherenkov angle at all distances, and at low frequencies near to the source. These two cases are examined individually in the following two sub-sections.

2.1. Behaviour near the Cherenkov angle

The condition 'near the Cherenkov angle' occurs when one of the $1-n\beta\cos\theta_n$ terms in the denominators of Eq. (2) and/or (3) tends to zero. In the endpoint approach, it is possible to observe one of the acceleration points such that $1-n\beta\cos\theta_0 \approx 0$ while $|1-n\beta\cos\theta_1| > 0$ (or *vice versa*), and one of the two terms can become arbitrarily large. In the ZHS formula however, the same denominator $1-n\beta\cos\theta_1$ applies to the whole formula — as it approaches zero, Eq. (3) tends to the following (finite) result:

$$\lim_{(1-n\beta\cos\theta_1)\to0}\vec{E}_{\rm zhs}(\vec{x},\nu) = 4\frac{Q}{c^2}\beta\sin\theta_1\frac{e^{ikR_1}}{R_1}\pi i\nu t_0\hat{E_1}. \qquad (5)$$

Eq. (5) is well-behaved, and reproduces the well-known characteristics of coherent Vavilov-Cherenkov radiation: coherency proportional to the track-length $\ell = 2c\beta t_0$, and a spectrum rising with frequency ν.

To illustrate this difference, the farfield electric fields calculated by both the ZHS and endpoint formulas for

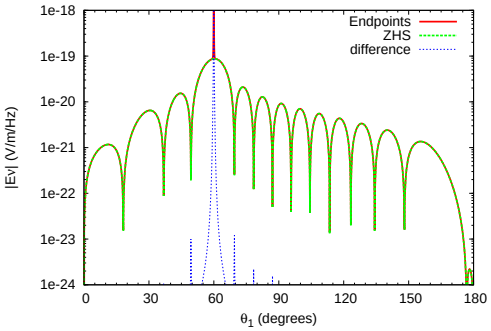

FIGURE 2. Radiated field $E(\nu)$ in the Tamm problem calculated according to both the endpoint (Eq. (2)) and ZHS (Eq. (3)) methods, and the absolute difference between them. The parameters used are: $\ell = 1$ m, $\beta = 0.999$, $R_1 = 1$ km, $n = 2$, and $\nu = 1$ GHz.

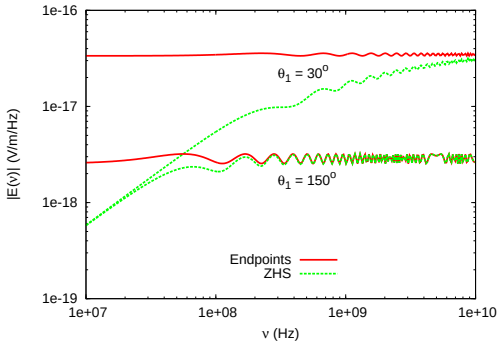

FIGURE 3. Radiated field magnitude $|E(\nu)|$ in the Tamm problem at two different viewing angles θ_1, calculated according to both the endpoint (Eq. (2)) and ZHS (Eq. (3), with 1000 sub-divisions) formulas. The parameters used are: $\ell = 1$ m, $\beta = 0.999$, $R_1 = 10$ m, $n = 2$.

the Tamm problem are plotted in Fig. 2 as a function of viewing angle. The agreement is better than 1% except when within 0.8° of the Cherenkov angle $\theta_C \approx 60^\circ$, and closer to that the endpoint solution tends (obviously, unphysically) to infinity.

2.2. Behaviour in the near-field

As an observer approaches the source track in the Tamm problem, the angles θ_n and distances R_n become significantly different, and the far-field assumption of the ZHS formula begins to break down. The standard solution to this is to divide the track into numerous sub-tracks, and apply Eq. (3) to each, summing the result. A simple test of whether the resulting division is sufficiently fine is to further sub-divide and check that the result is stable. Using this method, it is generally assumed that the ZHS formula can be applied to the near-field. In the case of the endpoint formulation however, there is no such thing as a 'near-field', because the radiation comes from two point-like sources, for which the distances and angles are calculated seperately. In the near-field of the Tamm problem, the particle in question will move significantly closer to, or further-away from, the observer, and this change should be observable at sufficiently low frequencies. However, a quick examination of Eq. (3) — or more obviously, (5) — reveals that the low-frequency limit of the ZHS formula is always 0, regardless of the nature of the sub-division. In the case of the endpoint formula however, a non-zero limit will always be obtained, since $R_0^{-1} \neq R_2^{-1}$ in general.

A comparison of the end-point and ZHS solutions in the near-field is given in Fig. 3, as a function of frequency for two viewing angles. The two methods agree reasonably well in the high-frequency range (there is a difference of magnitude), but diverge at low frequencies, with both exhibiting their characteristic behaviours. Note that unlike the far-field case, the direction of the field vectors will be different for the two different solutions.

The comparisons in the above section indicate that only in the far-field regime away from the Cherenkov angle will the ZHS and endpoint approaches prove equivalent, and it is generally presumed that this result is correct. Near the Cherenkov angle in the far-field, the divergence of the endpoint solution suggests an unphysical result, and the ZHS formula should therefore be the most trustworthy; conversely, in the near-field the low-frequency behaviour of the ZHS approach appears unphysical. However, the questions remain: does ZHS give the correct result in the far-field near the Cherenkov angle; does the endpoint approach give the correct result in the near-field far from the Cherenkov region; and, most importantly: what is the correct result for an arbitrary geometry? This last question will be answered in the following section. For further discussion as to the different natures of the endpoint and ZHS approaches, see the contribution by K. Belov in these proceedings [8].

3. A COMPLETE SOLUTION

In this section, a numerically-integrable expression for the complete solution to the Tamm problem is developed. A physically equivalent solution has been independently and simultaneously developed by García-Fernández et al. in Ref. [9], which also requires a numerical integration to solve, although the mathematical formulation differs. The approach used here follows closely the analysis of Afanasiev [10] in the case of an infinite track.

The key ingredients for a full treatment of the Tamm problem are a description of the source charge ρ (and

thus current $J = \vec{v}\rho$):

$$\rho(\vec{R},t) \;=\; Q\delta(x)\delta(y)\delta(z-vt)\mathscr{H}(t+t_0)\mathscr{H}(-t+t_0), \quad (6)$$

a definition of the Fourier transform, since this is the space in which the solution will be derived:

$$f(\vec{k},\omega) \;\equiv\; \int d^3\vec{r}\,dt\; f(\vec{r},t)\exp[-i(\vec{k}\cdot\vec{r}-\omega t)] \qquad (7)$$

and an expression for the potentials in this Fourier space (see e.g. Ref. [7]) in the Lorentz gauge:

$$\begin{aligned}\Phi(\vec{k},\omega) &= \frac{4\pi}{\varepsilon(\omega)}\frac{\rho(\vec{k},\omega)}{k^2-\frac{\omega^2}{c^2}\varepsilon(\omega)}\\ \vec{A}(\vec{k},\omega) &= \frac{4\pi}{c}\frac{\vec{J}(\vec{k},\omega)}{k^2-\frac{\omega^2}{c^2}\varepsilon(\omega)}.\end{aligned} \qquad (8)$$

Here, $\varepsilon(\omega)$ is the (in-general complex) permittivity. Using the definition of the Fourier transform in Eq. (7), and converting to cylindrical coordinates k_r, k_ϕ, k_z, $\rho(\vec{k},\omega)$ is found to be:

$$\rho(\vec{k},\omega) \;=\; -2Q\frac{\sin[t_0(k_z v-\omega)]}{k_z v-\omega} \qquad (9)$$

while only the z-component of J, and hence A, remains non-zero (and follows trivially from the above).

While simple, the expressions derived by combining Eq. (9) with Eq. (8) are not very useful to those of us who live in real Cartesian space: the expression for $\Phi(\vec{x},\omega)$ in cylindrical Cartesian coordinates r,ϕ,z is:

$$\begin{aligned}\Phi(\vec{x},\omega) &= \frac{-Q}{\varepsilon(\omega)\pi^2}\int dk_\phi\int dk_r\int dk_z \qquad (10)\\ &\quad\cdot\frac{k_r}{k_z^2+k_r^2-\frac{\omega^2}{c^2}\varepsilon(\omega)}\frac{\sin[t_0(k_z v-\omega)]}{(k_z v-\omega)}e^{i\Psi}\\ \Psi &\equiv xk_r\cos k_\phi + yk_r\sin k_\phi + zk_z.\end{aligned}$$

The expression for $A_z(\vec{x},\omega)$ follows similarly. It happens that the integration over k_ϕ can be solved exactly, to produce:

$$\begin{aligned}\Phi(\vec{x},\omega) &= -\frac{2Q}{\varepsilon(\omega)\pi}\int dk_r\int dk_z\frac{\sin[t_0(k_z v-\omega)]}{k_z v-\omega}\\ &\quad\cdot\frac{k_r}{k_z^2+k_r^2-\frac{\omega^2}{c^2}\varepsilon(\omega)}e^{izk_z}J_0(rk_r), \qquad (11)\end{aligned}$$

where J_0 is a Bessel function of zeroeth order[1]. Remarkably, the integral over k_r in Eq. 11 can also be solved exactly, for instance using result 6.532.4 from Ref. [11]; using this reduces Eq. 11 to the form:

$$\begin{aligned}\Phi(\vec{x},\omega) &= -\frac{2Q}{\varepsilon(\omega)\pi}\int dk_z\frac{\sin[t_0(k_z v-\omega)]}{k_z v-\omega}e^{izk_z}K_0(rq)\\ q^2 &= k_z^2-\frac{\omega^2}{c^2}\varepsilon(\omega), \quad \mathrm{Re}(q)>0 \qquad (12)\end{aligned}$$

Here, K_0 is a modified Bessel function of the second kind of zeroeth order, while the $\mathrm{Re}(q)>0$ condition in Eq. 12 — combined with the causality condition that $\omega\,\mathrm{Im}(\sqrt{\varepsilon(\omega)})>0$, and thus for normal media $\omega\,\mathrm{Im}(\varepsilon(\omega))>0$ — implies that q lies in the lower-right quadrant of the complex plane for positive frequencies, and in the upper-right quadrant for negative frequencies.

Expressions for the fields $\vec{E}(\vec{x},\omega)$ and $\vec{B}(\vec{x},\omega)$ can be calculated via the usual time-domain relations:

$$\begin{aligned}\vec{E}(\vec{x},t) &= -\vec{\nabla}\Phi(\vec{x},t)-\frac{\partial\vec{A}(\vec{x},t)}{c\,\partial t}\\ \vec{B}(\vec{x},t) &= \vec{\nabla}\times\vec{A}(\vec{x},t).\end{aligned} \qquad (13)$$

by writing $\vec{\nabla}$ and $\vec{\nabla}\times$ in cylindrical coordinates. Doing so requires first writing $\Phi(\vec{x},t)$ in terms of $\Phi(\vec{x},\omega)$ using the inverse Fourier transform (and similarly for $A(\vec{x},t)$) to obtain integral expressions for $\vec{E}(\vec{x},t)$ and $\vec{E}(\vec{x},t)$ in Eqs. (13); applying an inverse Fourier transform to both sides, and knowing the derivative $dK_0(x) = -K_1(x)dx$, then produces the following expressions for the field components:

$$\begin{aligned}E_r &= -\frac{2Q}{\varepsilon\pi}\int dk_z\frac{\sin[t_0(k_z v-\omega)]}{k_z v-\omega}e^{izk_z}qK_1(rq)\\ E_z &= \frac{2iQ}{\varepsilon\pi}\int dk_z\frac{\sin[t_0(k_z v-\omega)]}{k_z v-\omega}\\ &\quad\cdot\left(k_z-\beta\varepsilon\frac{\omega}{c}\right)e^{izk_z}K_0(rq) \qquad (14)\\ B_\phi &= -\frac{2\beta Q}{\pi}\int dk_z\frac{\sin[t_0(k_z v-\omega)]}{k_z v-\omega}e^{izk_z}qK_1(rq).\end{aligned}$$

The other three components are zero.

The expressions in Eq. 14 are exact solutions to the Tamm problem in the frequency-domain. They allow for a frequency-dependent refractive index, although for radio applications the frequency-dependence is not required to obtain physically-relevant results. The charge is considered point-like, and the medium homogeneous, but this is the same standard approximation that is made with all macroscopic calculations, and would likely only prove a limitation in the ultra-violet regime. The use of a non-magnetic medium is appropriate to all media so-far considered for radio applications. Thus it is completely general in the regime of Classical electrodynamics. Criticisms of the value of this type of calculation often hinge on the (obviously unphysical) infinite acceleration at the end-points implied by the Tamm problem,

[1] The integral over k_ϕ is equivalent to one of the many definitions of J_0

or the constant-velocity assumption. The answer to this is that it is the role of the program (and hence programmer) generating the particle track segments to which the Tamm solutions are applied to ensure that the tracks approximate the true motion 'sufficiently well', in which case the exact solutions given by Eqs. (14) to the Tamm problem will approach the exact solutions to the true particle motion which the Tamm problem approximates.

4. NUMERICAL EVALUATION

The exact solutions to the Tamm problem given in Eqs. (14) do not have analytic solutions for an arbitrary observer at position (r,ϕ,z) observing at angular frequency ω. At large values of $|k_z|$, the magnitudes of the modified Bessel functions K_0 and K_1 fall off exponentially, which allows a finite numerical integration regime. The expressions contain no singularities provided that the complex nature of $\varepsilon(\omega)$ is retained[2], though for some geometries and transparent media a sharp peak in the integrand near $k_z = \mathrm{Re}(\varepsilon)^{0.5}\frac{\omega}{c}$ must be treated carefully. Here, *Mathematica 8.0* was used to evaluate the integrals.

In Fig. 4, the Tamm problem has been evaluated numerically using the exact solution, and the endpoints and ZHS solutions, for approximately characteristic geometries in air-shower detection experiements such as LOPES. The agreement between the exact calculation and the ZHS result is near-perfect in this range, only diverging slightly for very small values of the radial distance r. Again, the endpoint solution is correct everywhere except near ~ 200 m, where it encounters the Cherenkov divergence.

5. CONCLUSION

An exact formula for the solution to the Tamm problem has been derived in Eq. 14. Using it, it is shown that the ZHS solution to the Tamm problem is correct at all but very low frequencies and very near geometries which are currently not of experimental significance, while the endpoint solution also fails very near to the Cherenkov angle. Both methods agree, and produce the correct result, in the far-field regime at which most calculations are produced. Importantly, current methods used in simulation codes to overcome the respective flaws of the methods — divergence at the Cherenkov angle for endpoints, track sub-division for ZHS — are completely consistent with the exact solution. Investigations into the optimum trade-off between the accuracy of ZHS near the Cherenkov angle, and the speed of calculation of the endpoints method away from it, are still ongoing.

[2] While a logarithmic singularity does appear in E_z for the case of a vacuum and $\beta \neq 1$, this situation has already violated the condition $\mathrm{Re}(q) > 0$ in Eq. (12), and so must be treated separately.

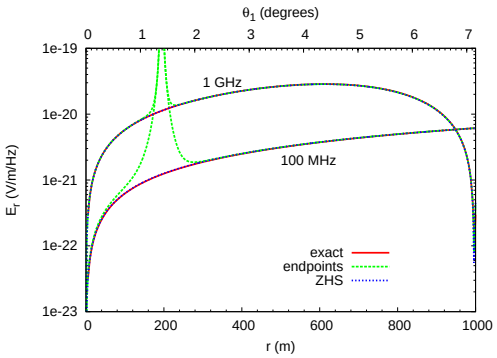

FIGURE 4. Radiated field magnitude $|E(\nu)|$ in the Tamm problem at two frequencies as a function of radial offset r $(= R\cos\theta_1)$ for a characteristic air-shower geometry: $R \sim z =$ 8 km, $n = 1.0003$, $\ell = 40$ m, $\beta = 0.999995$ (electron energy ~ 160 *MeV*, and $\mathrm{Im}(\varepsilon) \to 0$.)

ACKNOWLEDGMENTS

C.W. James acknowledges T. Huege of the Karlsruhe Institute of Technology for his help in the numerical evaluation of the integrals presented in this paper.

REFERENCES

1. I.M. Frank and I.E. Tamm, *Dokl. Akad. Nauk SSSR* **14**, 109 (1937).
2. I.E. Tamm, *J. Phys. Moscow* **1**, 439 (1939).
3. E. Zas, F. Halzen, and T. Stanev, *Phys Rev D* **45**, 362 (1992).
4. J. Alvarez-Muñiz, W.R. Carvalho, and E. Zas, *Astroparticle Physics* **35**, 324–341 (2012).
5. M. Ludwig and T. Huege, *Astroparticle Physics* **34**, 438 (2010).
6. C. James, H. Falcke, T. Huege, and M. Ludwig, *Phys. Rev. E* **85**, 056602 (2011).
7. J.D. Jackson, *Classical Electrodynamics* (3rd ed), John Wiley & Sons, New York, 1998, p. 656.
8. K. Belov, "Radio emission from Air Showers. Comparison of theoretical approaches.", in *Proceedings of the ARENA 2012 workshop (Erlangen, Germany)*, AIP Conference Proceedings, to be published.
9. D. García-Fernández, J. Alvarez-Muñiz, W.R. Carvalho, Jr, A. Romero-Wolf, E. Zas, eprint arXiv 1210:1052 (2012).
10. G.N. Afanasiev, *Vavilov-Cherenkov and Synchrotron Radiation*, Kluwer Academic Publishers, Dordrecht, 2004, pp. 127–207.
11. I.S. Gradshteyn and I.M. Ryzhik, *Table of Integrals, Series, and Products* (6th ed.), A. Jeffrey and D. Zwillinger (eds), Academic Press, Salt Lake City, 2000.